ON OBTAINING BINARY POLYELECTROLYTE COMPLEXES OF CHITOSAN *BOMBYX MORI* WITH COLLAGEN

Noira Rakhimovna Vokhidova[1,a,*], Shuhrat Shamsiddinovich Khudoyberdiyev[2,b], Ilnar Nakipovich Nurgaliev[1,c], Sayyora Sharafovna Rashidova[1,d]

[1] – Institute of Chemistry and Physics of Polymers of Scientific Academy of Uzbekistan, Tashkent 100128, Uzbekistan
[a] – ORCID: 0000–0003–0477–3708, [c] – ORCID: 0000–0002–6983–4375,
[d] – ORCID: 0000–0003–1667–4619
[2] – Bukhara State University, Bukhara 200114, Uzbekistan
[b] – ORCID: 0000–0002–0696–3743
[*]corresponding author: noira_vokhidova@yahoo.de

Abstract

We obtained binary polyelectrolyte complexes containing chitosan from Bombyx mori and collagen with a mass ratio of 10:1; 10:2, and 10:3. During the interaction between the macromolecules, due to the compensation of the positive charges of chitosan with the negative charges of collagen, the zeta potential of the solutions of polyelectrolyte complexes changed from +15.2 to +5.67 mV. We revealed the dependence of the size characteristics of the particles of polyelectrolyte complexes on time and the ratio of macromolecules. An examination of the morphology of the films of polyelectrolyte complexes demonstrated that in the evaluated chitosan/collagen mass ratios, non-spherical nanosized particles up to ≤ 60 nm form on the surface of the films. We evaluated the mechanism of formation of complexes by using Fourier-transform infrared spectroscopy and confirmed the findings with density functional theory and molecular dynamics. We found that the particle diameter is inversely proportional to the diffusion coefficient. The results show that the particles are almost uniformly distributed over the surface of the polymer matrix and have a unimodal character. We obtained reproducible results when using a chitosan/collagen mass ratio of 10:2 to dye natural silk. We found that the complexes contribute to increase the intensity and stability of colour relative to soap and friction.

Keywords: *chitosan, collagen, binary complex, diffusion coefficient, hydrodynamic radius, staining intensity*

Received: 15.02.2023
Accepted: 23.03.2023

1. Introduction

In recent years, there has been an increase in the demand for new materials based on polyelectrolyte complexes (PEC). For this purpose, scientists have focused on the specific properties of chitosan (CS) complexes with other polyanions. PEC represent a special class of polymeric substances formed as a result of cooperative reversible reactions of the combination of oppositely charged ions [1, 2].

Interactions between collagen and CS can occur via the –OH, $–NH_2$, and –COOH groups in collagen, which are able to form hydrogen bonds with the –OH and $–NH_2$ groups in CS. In addition, at pH < 6.5, most of the amino groups of CS are protonated, which contributes to the formation of electrostatic bonds between the NH_3^+ groups of CS and the $–COO^–$ groups of aspartic and glutamine residues in collagen [3, 4].

CS PEC tend to aggregate due to charge neutralisation. Therefore, to avoid aggregation and to control the size of nanoparticles, at least two conditions are mandatory: polyelectrolyte solutions must be diluted, and one of the polyions must be in excess so that the following inequality is preserved: (n+/n–) ≠1 (Figure 1) [5].

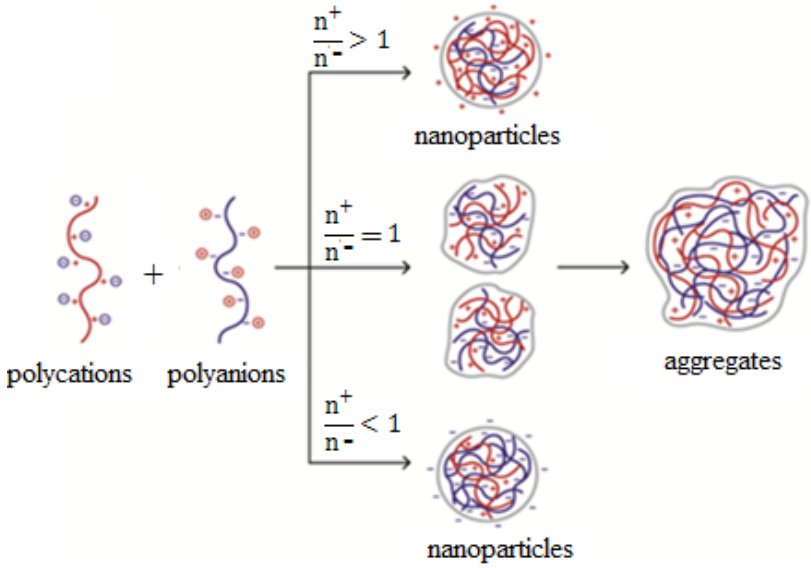

Figure 1. The influence of the charge ratio of polyelectrolytes on the size and charge of the formed polyelectrolyte complexes [5].

If the charge ratio is greater or less than unity, then the resulting nanoparticles are charged with the same charge as the polyion in excess. Experiments have shown that at $n^+/n^– = 1$, uncharged particles are formed, and as a result of agglomeration, large aggregates are formed.

The formation of PEC is the result of Coulomb interactions between oppositely charged polyelectrolytes, which leads to interpolymer ionic condensation. The driving force arises mainly due to the release of molecular counterions into the solution phase, which increases the entropy of the system. In addition, intermolecular interactions, such as chemical and physical bonds, are also involved in the formation of PEC. The formation of PEC usually includes two or three stages (Figure 2).

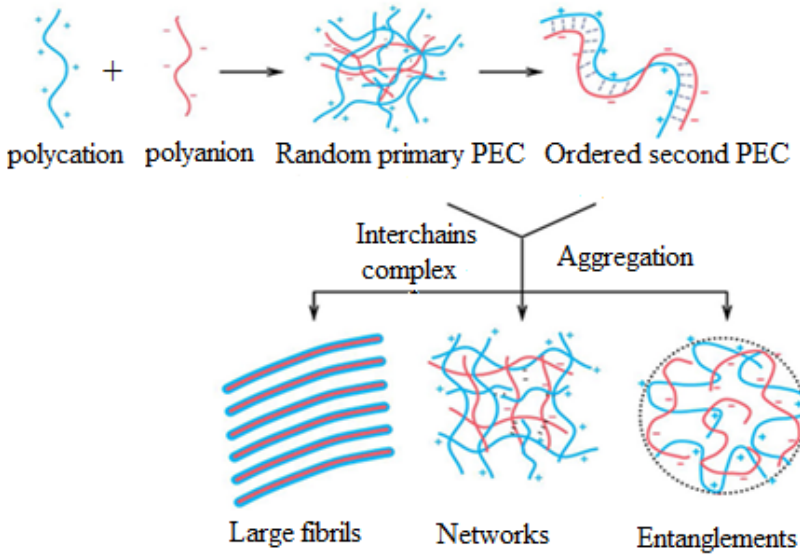

Figure 2. A scheme for the formation of polyelectrolyte complexes (PEC) [6].

To regulate the composition and structures of inter-PEC, it is advisable to vary the synthesis conditions. According to Wu *et al.* [6], the first stage proceeds instantaneously and leads to the formation of a random primary complex with significant distortions in the configuration of the polymer chains. Then the secondary complex is formed by rearranging the existing bonds within the complexes.

CS, a biocompatible positively charged polysaccharide derived from renewable sources, is considered a promising polymer for medical use. Despite the high application potential of CS, its susceptibility to the presence of ions, pH-dependent solubility, insufficient rheological properties, and film brittleness can be a serious limitations to its potential applications. Among modifications of CS, researchers have paid particular attention to PEC spontaneously formed by mixing CS with oppositely charged polymers under mild synthesis conditions [7]. CS can be easily modified due to its molecular chain, which contains a large number of active amino and hydroxyl groups, through various modifications [8].

Do Mai Train *et al.* [9] prepared a nanosized polymer system based on CS and fish squamous collagen by emulsification for the delivery of lovastatin, a drug used to lower blood cholesterol concentrations. A hydrogel based on CS/collagen was obtained by lyophilisation at 20°C for 12 h, with a 1:1 mass ratio of polyelectrolytes. After that, the authors immersed frozen samples in a pre-chilled sodium hydroxide/ethanol solution and incubated it at –20°C for 24 h. Then the samples were removed from the freezer and washed three times with 50% ethanol. At the end, the samples were washed with water until the pH was 7. The authors then immersed the samples in a 99.8% ethanol for 1 h and dried them at 22°C [10, 11].

The interaction between CS and alkaline gelatine during PEC formation has been examined with scanning electron microscopy (SEM). The authors found that for CS/gelatine mass ratios from 0.1 to 1.5, PEC are formed due to intermolecular hydrogen bonds [12].

With electrospinning, researchers have obtained nanofibres based on gelatine/CS–poly(ethyleneoxide) (PEO) at various mass ratios (9:1, 8:2, 7:3, and 6:4) in the presence of 50% (v/v) acetic acid as a solvent. The tensile strength, Young's modulus, and elongation at break were 0.76–1.70 MPa, 21.0–31.7 MPa, and 22.3%–27.4%, respectively. In particular, membranes based on a gelatine/CS–PEO mass ratio of 7:3 had excellent properties, demonstrating great potential for use in skin regeneration [13, 14]. Hydrogels based on 75:25 (vol.%) CS/collagen showed a crystalline structure and mechanical strength closer to the mechanical strength of bone and could be applied in the field of bone tissue engineering and regenerative medicine [15]. CS has unique chemical properties owing to its cationic charge in solution. Despite the wide applicability of CS to various fields, it has rarely been used to dye textile materials due to the lack of technology [16].

PEC can form biocompatible matrices and can be used in various industries. In this regard, we aimed to identify the conditions for the synthesis of PEC based on CS isolated from the pupae of the silkworm *Bombyx mori* and collagen isolated from cattle skin. We investigated the physicochemical properties of binary PEC and the possibility of their use in dyeing natural silk.

2. Materials and Methods

CS from *B. mori* was obtained according to a previous study [17]. The molecular mass of CS is 1.98×10^5 g/mol and the degree of deacetylation is 85%. Collagen was obtained from cattle skin [18] and purified from low-molecular-weight salts by membrane dialysis [19]. The degree of purification was 90%.

Static light scattering and dynamic light scattering (DLS, also known as photon correlation spectroscopy, Photocor Compact, Russia) was performed. The range of measured sizes is from fractions of nanometres to 5–10 μm. The laser power of the apparatus was 2–35 mW. Photocor analysers have a mode that allows automatic measurements, processing, and presentation of the results.

The Litesizer 100 (Anton Paar GmbH, Austria) particle size analyser was used to measure the size of ultrafine particles in liquid solutions, determined from the Einstein-Stokes equation by the diffusion coefficient. The diffusion coefficient is calculated from the characteristic fluctuation time of the intensity of light scattered by particles. The autocorrelation function contains information about the diffusion coefficient, which makes it possible to obtain the desired hydrodynamic radius, which is a model of the particle size. The light source was a 658 nm laser from a 40 mW single-frequency laser diode.

The dynamic viscosity of CS and collagen solutions as well as PEC based on them was determined with a Viskotester 2 plus rotational viscometer (HAAKE, Germany). The electrokinetic potential on the surface of PEC particles was determined by the method of dynamic quasi-elastic light scattering of polymer solutions on a Zetasizer Nano ZS instrument (Malvern Instruments Ltd, United Kingdom).

Fourier-transform infrared (FTIR) spectroscopic studies of the obtained samples were carried out on a Brucer spectrometer (Germany). The IR Tracer-100 was characterized by a high signal-to-noise ratio of 60000:1, a resolution of 0.25 cm^{-1}, and the ability the work in fast scanning mode with the registration of up to 20 spectra per second.

Morphology of systems was investigated on an atomic force microscope (AFM) Agilent-5500 (USA) at room temperature. Maximum field of scanning at AFM by X, Y was 15x15 micrometer square and 1 micrometer for Z.

The morphology of the PEC films was evaluated using an Agilent 5500 atomic force microscope (USA) at 22°C. The analysis used silicon cantilevers with a hardness of 9.5 N/m and a frequency of 145 kHz. The maximum scanning area was 15 × 15 μm^2 for X and Y and 1 μm for Z.

The degree of the change in the colour characteristics of fabrics after dyeing was carried out in standard D65 radiation on an X-Rite Ci7800 laboratory spectrophotometer (Korea) [20]. This approach is recommended when measuring the colour of luminescent samples because the distribution of the radiation flux in the ultraviolet (UV) region of its spectrum is normalised [21].

Computational methods: The theoretical objective of the current work is to investigate the interaction of CS with collagen using the DFT method to be a primer for understanding the interaction to validate literature experimental results theoretically. A monomeric link was taken as the structural unit of CS, and the structural unit of collagen was taken as Asparagine and Glutamine.

The calculations were performed using the GAUSSIAN 09 package [22] and the Gaussview 5.0.9 molecular visualization program using DFT with the standard set basis 6–31++G (d,p) [23]. The first stage of the theoretical calculation was the determination of the optimized molecular structures of CS and amino acids (AA). The charges of atoms are calculated, and diagrams of boundary molecular orbitals are constructed: the highest occupied (HOMO) and lowest unoccupied (LUMO) molecular orbitals and their energies are determined. Interactions of CS with AAs were studied using reactivity descriptors. A monomeric link was taken as the structural unit of CS; in calculations in the gas phase, AAs are considered a nonionic form due to the greater intrinsic affinity for the proton of the carboxylate oxygen atom compared to the nitrogen atom of the amino group. The interaction energy (ΔE_{inter}) is calculated using the equation-based approach:

$$\Delta E_{\text{inter}} = E_{CS\text{-}AA} - (E_{CS} + E_{AA}) + E_{BSSE}$$

where $E_{CS–AA}$, $E_{CS,}$ and E_{AA} are the energy of the complex, CS, and AAs, respectively. E_{BSSE} is a base set superposition error (BSSE) correction calculated using the direct difference method for calculating molecular interactions based on a bivariate trans-correlation approach together with special methods for estimating other errors [24].

3. Results and Discussion

3.1. DLS

We prepared PEC by mixing a 0.08% solution of CS and a 0.05% solution of collagen at specific mass ratios. Using DLS, we determined the hydrodynamic diameters of PEC particles obtained for each of the CS/collagen mass ratios (Table 1 and Figure 3).

Table 1. The dependence of the hydrodynamic particle size of polyelectrolyte complexes on the chitosan/collagen mass ratio (the solvent was acetate buffer, pH 6.3).

No.	Chitosan/collagen mass ratio	d [nm]	d [μm]
1	10:1	218 (19.5%)	34 (80.5%)
2	10:2	455 (35.3%)	48 (61.7%)
3	10:3	378 (28%)	58 (72%)

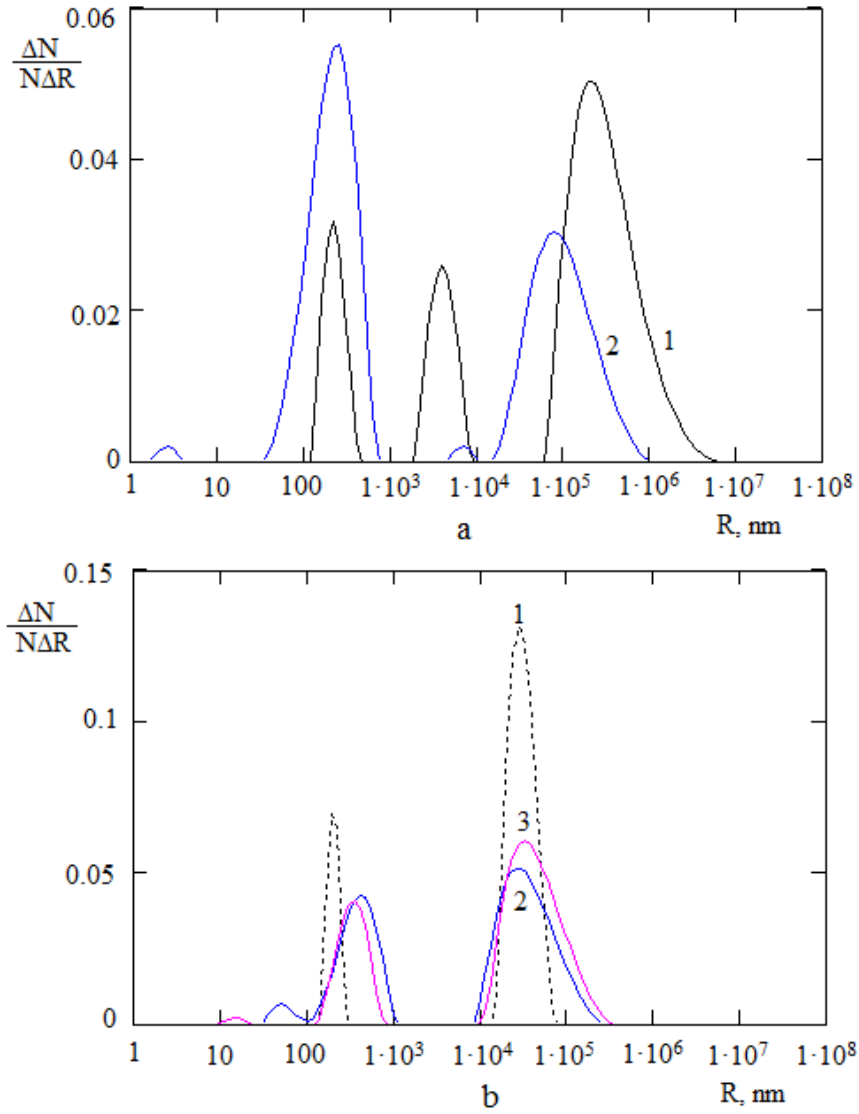

Figure 3. The hydrodynamic size and distribution of (top, a) particles of (1) chitosan and (2) collagen and (bottom, b) polyelectrolyte complexes of various chitosan/collagen mass ratios, namely (1) 10:1, (2) 10:2, and (3) 10:3.

According to Figure 3a, the particle size distribution of the initial polymers has a polymodal character and is mainly located in the micron range. As can be seen from Figure 3b, regardless of the CS/collagen mass ratio, there is a decrease in the number of peaks to two distribution areas. The decrease in the reaction system of charged functional groups with a CS/collagen mass ratio of 10:2 leads to agglomeration of PEC particles. These data are in good agreement with the literature [5].

3.2. Hydrodynamic Characteristics of PEC Prepared with CS and Collagen

We next determined the hydrodynamic parameters of PEC formed by mixing solutions of 0.5% CS and 0.5% collagen in acetate buffer (pH 6.3) at a mass ratio of 10:1, 10:2, and 10:3 (Figure 4).

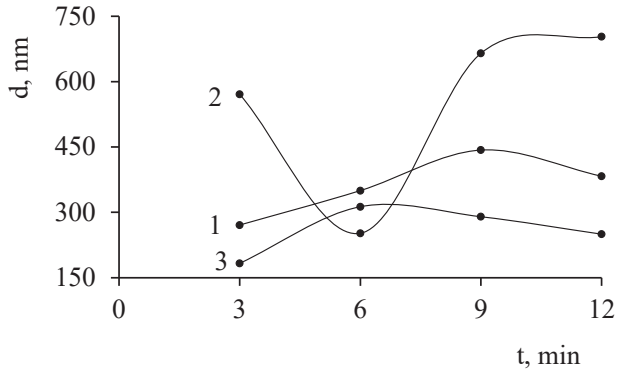

Figure 4. The effect of time on the hydrodynamic dimensions of polyelectrolyte complexes of various chitosan/collagen mass ratios, namely (1) 10:1, (2) 10:2, and (3) 10:3.

We examined the influence of time on the hydrodynamic dimensions of PEC and found that the interaction between macromolecules proceeded for 10 ± 2 min, after which time the particle sizes showed almost no change. When the CS/collagen mass ratio was 10:2, the hydrodynamic diameters of the particles decreased from 570 to 250 nm, and after 6 min of interaction they increased to 700 nm. Accordingly, within 3–12 min at the CS/collagen mass ratios of 10:1 and 10:3, the hydrodynamic sizes of PEC particles initially increased slightly from 180 to 250 nm and from 270 to 380 nm, respectively, but after 9 min there was a slight decrease. This change could be due to intra- and intermolecular hydrogen and electrostatic bonds in solutions of these macromolecules. At the CS/collagen mass ratio of 10:1, the hydrodynamic diameter of CS particles decreases, although increasing the mass of collagen in the system leads to its sharp increase, which is probably due to the appearance of collagen macromolecules in the system.

It should be noted that one of the most important parameters of PEC particles is the diffusion coefficient, the value of which is inversely proportional to the hydrodynamic radius of the particles (Figures 5 and 6).

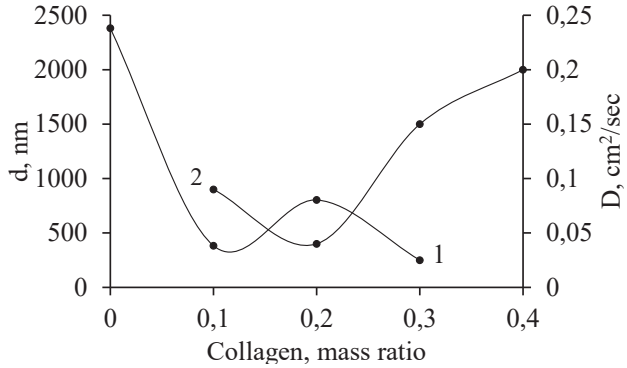

Figure 5. The dependence of (1) the particle size and (2) the diffusion coefficient of polyelectrolyte complexes on the chitosan/collagen mass ratio. The solvent was acetate buffer (pH 6.3) and τ is 12 min. Note that in the chitosan/collagen mass ration, chitosan remained constant at 10.

According to the measurement results, during the formation of PEC, the hydrodynamic diameter of the particles decreased by a factor of 5 compared with the initial polyelectrolytes. However, PEC particles at a CS/collagen mass ratio of 10:2 were reduced to 2.5 times. This mass ratio produced the highest diffusion coefficient, a finding that is logical (Figure 6).

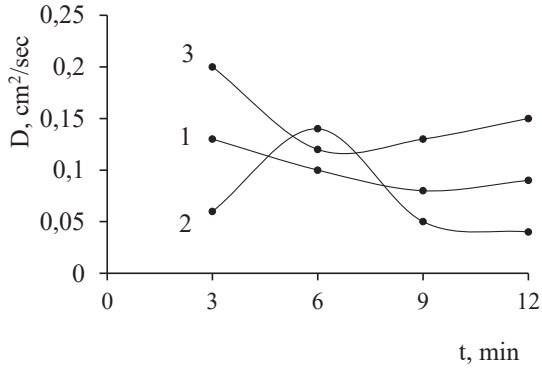

Figure 6. The influence of the interaction time between chitosan macromolecules and collagen on the diffusion coefficient of polyelectrolyte complex particles formed with a chitosan/collagen mass ratio of (1) 10:1, (2) 10:2, and (3) 10:3.

As Figure 6 shows, the dependence was non-linear. For the PEC particles formed with a CS/collagen mass ratio of 10:1 and 10:3, from 3 to 12 min of interaction, the diffusion coefficient changed slightly by 1.44 and 1.33 times, respectively. For the PEC particles formed with a CS/collagen mass ratio of 10:2, the diffusion coefficient was 0.06 at 3 min, 0.14 at 6 min, and 0.04 at 12 min. These differences are due to changes in the particle size during the selected time interval and the formation of relatively monodisperse PEC particles at this mass ratio.

Table 2. The dependence of the dynamic viscosity and zeta potential of solutions on the composition of polyelectrolyte complexes formed from chitosan and collagen (the solvent was acetate buffer, pH 6.3).

No	Components and mass ratio	μ [dPa·s]	Zeta ζ potential [mV]
1	Chitosan	13	+15.2
2	Collagen	69	–1.88
3	Chitosan/collagen = 10:1 (Q (+))	11	+11.7
4	Chitosan/collagen = 10:2 (Q (+))	19	+8.47
5	Chitosan/collagen = 10:3 (Q (+))	17	+5.67

We determined the dynamic viscosities of the initial polyelectrolytes as well as the binary PEC based on them (Table 2). It should be noted that during the formation of binary PEC, the introduction of a small amount of collagen into a solution containing CS led to a marked (5–6 times) decrease in the dynamic viscosity of the solution. PEC formed with a CS/collagen mass ratio of 10:2, the dynamic viscosity was 19 dPa·s, which is more than the other PEC.

The zeta potential of CS at pH 6.3 was positive (+15.2 mV), while the zeta potential of the collagen solution was negative (–1.88 mV, isoelectric point equal to 6) (Table 2).

When collagen, which contains negatively charged –COOH groups, was added to CS, the zeta potential decreased from +15.2 to +5.67 mV. Thus, we have developed a technique to obtain binary PEC.

3.3. Fourier-Transform Infrared Spectroscopy (FTIR) Spectroscopy

We obtained films of CS, collagen, and their PEC at 22°C by dry moulding. The FTIR spectrum of *B. mori* CS (Figure 7) shows the following bands: 3358 cm^{-1} (–OH and –NH), 1653 cm^{-1} (ν=(C=O); amide I), 1572 cm^{-1} (ν=(C=O, C–N and δ=(NH); amide II), 1421 cm^{-1} (δ=(O–H), 1375 cm^{-1} (δ=(CH_3), and 1151 cm^{-1} (ν=(C–O–C). These absorption bands are all characteristic of the functional groups present in CS.

The FTIR spectrum of collagen (Figure 7) shows the following bands: 3288 cm^{-1}, which corresponds to the vibration of the amide group (ν=(NH)), 2935 cm^{-1} (ν=(CH); 1635 cm^{-1}, which indicates the stretching vibration of the carbonyl group (ν=(C=O); amide I); 1521 cm^{-1} (ν=(C=O, C–N and δ=(NH); amide II)); and 1448 cm^{-1} (ν=(N–C–O); amide III). These bands are characteristic of collagen.

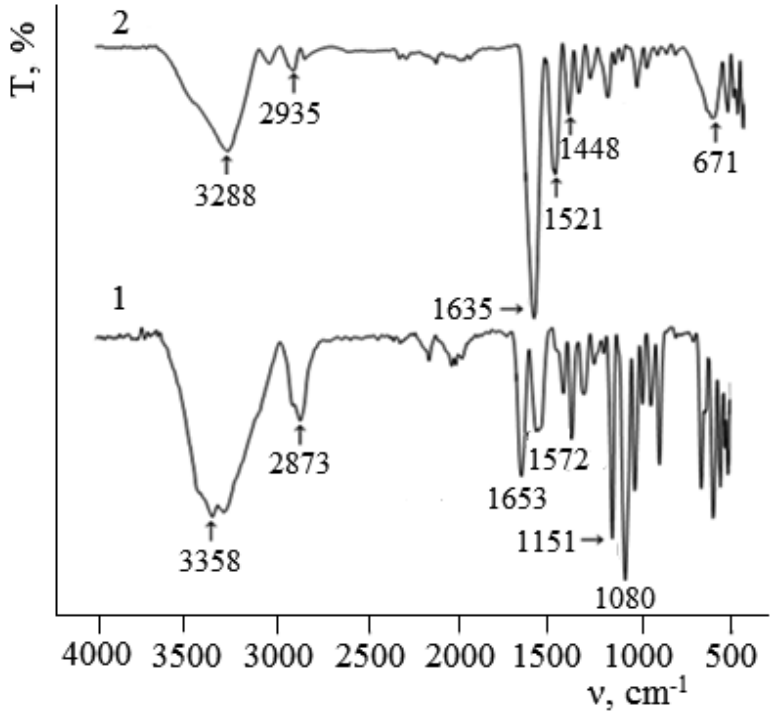

Figure 7. Fourier-transform infrared spectra of (1) chitosan and (2) collagen.

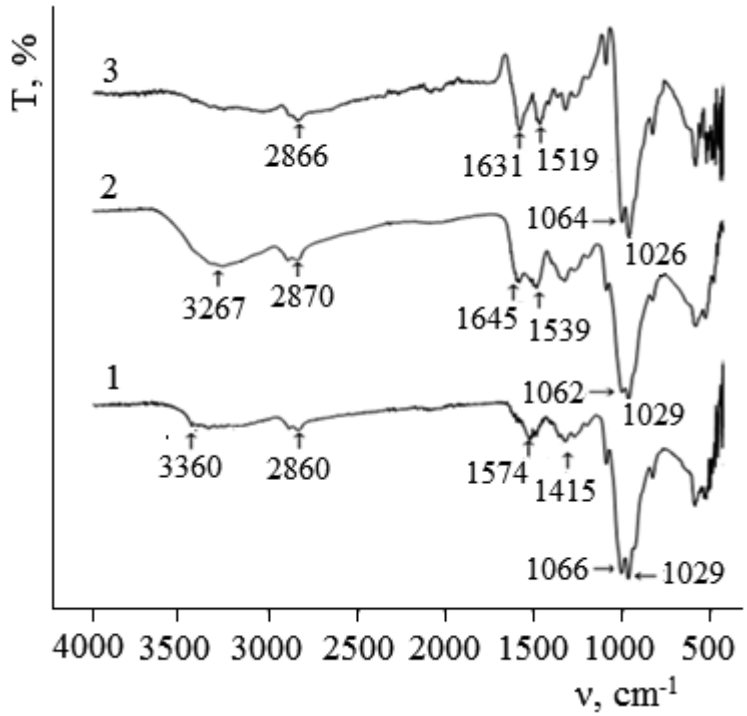

Figure 8. Fourier-transform infrared spectra of polyelectrolyte complexes formed from a chitosan/collagen mass ratio of (1) 10:1, (2) 10:2 and (3) 10:3.

Figure 8 shows the FTIR spectra of PEC formed with a CS/collagen mass ratio of 10:1, 10:2, and 10:3. In contrast to CS, the spectrum of PEC formed with a CS/collagen mass ratio of 10:1 exhibits some shifts and an increase in the intensity of absorption bands at 3360 cm^{-1} (ν=(O–H)), 2860 cm^{-1} (ν=(CH_3)), 1574 (ν=(COO^-); amide I), 1415 cm^{-1} (δ=($^+NH_3$); amide II), and 1379 cm^{-1} (ν=(N–C–O); amide III).

Compared with the CS spectrum, the spectrum of the PEC formed with a CS/collagen mass ratio of 10:2 also shows some shifts and an increase in the intensity of absorption bands at 3267 cm^{-1} (ν=(O–H)), 2870 cm^{-1} (ν=(CH_3)), 1539 cm^{-1} (δ=($^+NH_3$); amide II), 1381 cm^{-1} (ν=(N–C–O); amide III), and a weak shoulder at 1645 cm^{-1} corresponding to stretching vibrations (ν=(COO^-); amide I). This is probably due to the interaction between collagen and the CS amino groups.

Finally, in contrast to the CS spectrum, the spectrum of PEC formed with a CS/collagen mass ratio of 10:3 shows some shifts and an increase in the intensity of absorption bands at 2866 cm^{-1} (ν=(CH_3)), 1631 cm^{-1} (ν=(COO^-); amide I), 1519 cm^{-1} (δ=($^+NH_3$); amide II), and 1377 cm^{-1} (ν=(N–C–O); amide III). Overall, the bands indicating the vibrations for amide II are significantly shifted in the PEC, although the absorption bands of stretching vibrations are stable.

3.4. Atomic Force Microscopy (AFM) of PEC Films

Chitosan/collagen PEC films with various mass ratios were obtained by dry molding. from aqueous acetic solutions. The morphology of PEC were evaluated with AFM (Figure 9).

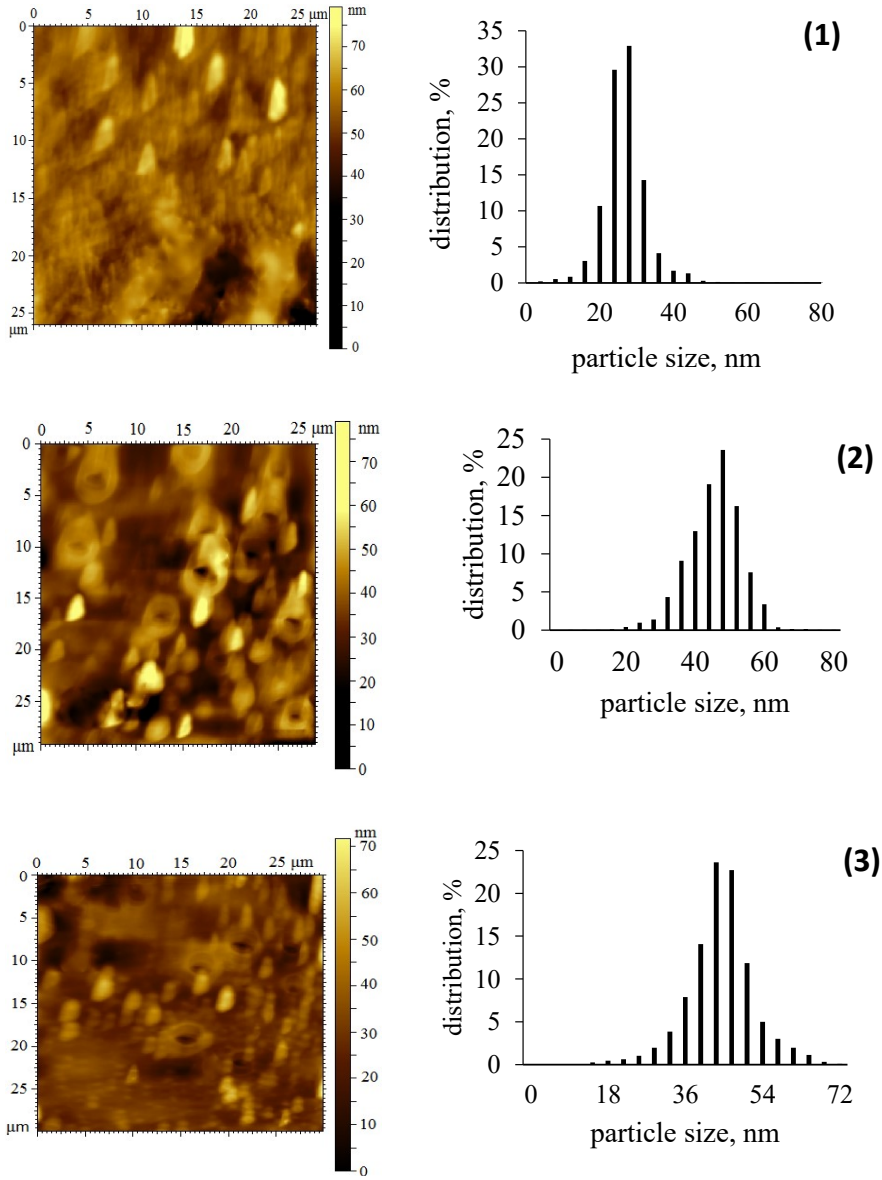

Figure 9. Atomic force micrographs and histograms of the distribution of chitosan/collagen particles on the surface of the polymer matrix. The polyelectrolyte complexes were formed with a chitosan/collage mass ratio of (1) 10:1, (2) 10:2, and (3) 10:3.

Regardless of the interval of the initial macromolecules under the chosen synthesis conditions, we noted that non-spherical nanoparticles with an average size of up to approximately ≤ 60 nm, which are unimodal, formed on the surface of the films. Specifically, for the CS/collagen mass ratio of 10:1, 10:2, and 10:3, the nanoparticles are 15–35, 25–60, and 32–50 nm, formed in one direction, and are relatively evenly

distributed on the surface of the polymer matrix. In general, the size of PEC particles is consistent with the DLS data. However, the AFM results also show that, despite the large size, the visible part of the PEC particles is uniformly distributed on the surface of the films.

3.5. Theoretical Calculations of the Formation of Inter-PEC

Theoretical calculations allow evaluating interactions between compounds to explore the possibility of forming various kinds of bonds, complexes, agglomerates, clusters, and nanostructures. We investigated the charge distribution of amino groups in CS chains of different lengths depending on the degree of deacetylation, the reactivity of the acetamide and amino groups in the CS composition, the interaction between CS and collagen, and the stability of their interpolymer complexes.

The calculated group charge distribution for the tertiary hydrogen atom of the protonated amino group of CS is 1.54 e [25]. These values indicate that these hydrogen atoms tend to form hydrogen bonds with electronegative centers. Similarly, a 1.55 e. group charge for an oxygen atom in Asparagine and 1.56 e. for an oxygen atom in Glutamine allowed us to evaluate the atypical CS–AA interaction between electronegative atoms with $–COO^-$ and $–NH_3^+$ CS group. The optimized structure of the complexes under consideration is shown in Figure 10.

The DFT calculations showed the presence of hydrogen bonds between the nitrogen atom of the amino group of CS and the O atom of the $–COO^-$ groups of the studied amino acids (Table 3). According to Table 3, the distance between the H atom of the $–NH_3^+$ –group of CS and the O atom of the $–COO^-$ groups of AAs is in the range of 1.001 Å (Asparagine) and 0.999 Å (Glutamine) which is typical for hydrogen bonds [26]. This indicates that CS forms hydrogen bonds with amino acids during the formation of complexes. Various protonation states of the complexes were tested as starting points for geometry optimization. The results have not confirmed the proton transfer complexes. Cationic or anionic AAs are well known for their ability to form hydrogen bonds with oppositely charged species [27]; however, the formation of such a salt bridge in the gas phase of the complexes under consideration was not observed. A high value of ΔE_{inter} promotes strong binding between CS and AAs in the complex, while a decrease in energy values promotes the dissociation of the complex.

Moreover, based on the ΔE_{inter} values, the suitability of the carrier to a particular AA can be assessed. The calculated values of ΔE_{inter} in gas and aqueous phases are presented in Table 3. The ΔE_{inter} is negative in all cases, contributing to complexes' formation. A high value of ΔE_{inter} for CS–Glutamine may be due to the strong Coulomb force of attraction, which leads to hydrogen migration. The charge of the O atom in $–COO^-$ group of Glutamine is more negative (–0.64 e) than that of Asparagine (–0.62 e).

Table 3. Hydrogen bond distance and BSSE corrected interaction energy of CS with AAs

Complex	H–H bond length between N…O [Å] (Aqueous phase)	$\Delta E_{inter.}$ [kkal/mol] (Gas phase)	$\Delta E_{inter.}$ [kkal/mol] (Aqueous phase)
CS–Asparagine	1.001	–89.51	–18.96
CS–Glutamine	0.999	–105.49	–23.1

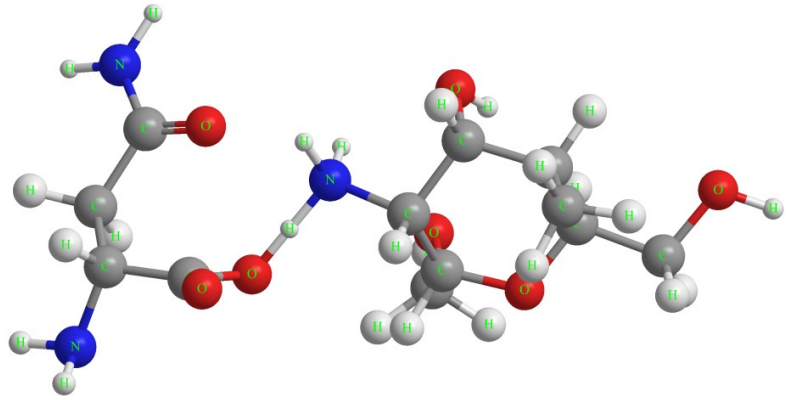

CS-Asparagine

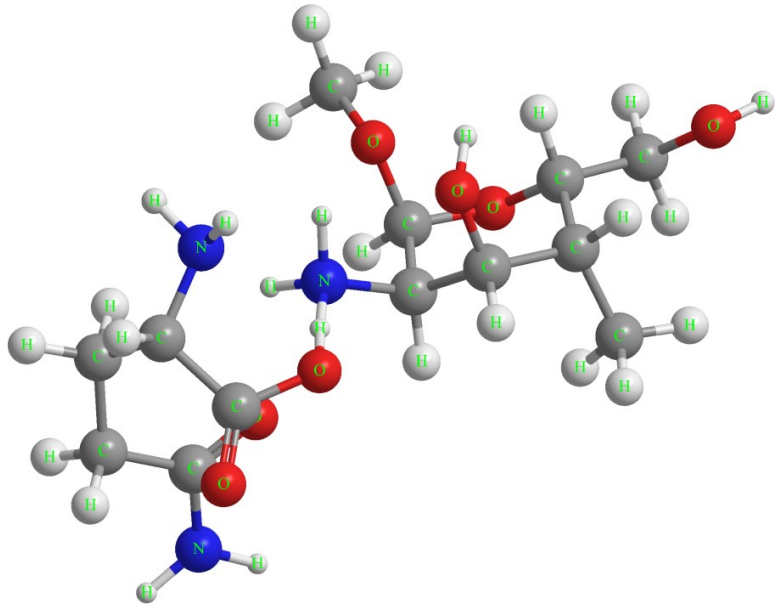

CS-Glutamine

Figure 10. Optimized geometries of CS complexes with AAs

The formation of CS-Collagen complexes was carried out in the aqueous phase. As the interaction energy is of decisive importance for the biomedical applications of such complexes, thus we simulate the behavior of the passage of complexes through the cellular media of living organisms by calculating the effect of the aqueous phase on the interaction. As seen in Table 3, the aqueous phase primarily affects the interaction energy of these systems. There is a progressive destabilization of CS complexes with AAs. The results show that molecules with opposite charges are indeed more separated and more stable than complexes in water, leading to a decrease in ΔE_{inter}.

This can also be explained by the fact that in polar environments, the interaction with the environment (solvation) is probably more important than the electrostatic interaction

between the two interacting molecules, leading to their preferential stabilization. Due to the solvation of positively charged fragments, the repulsive interaction between them decreases, which can increase the strength of the hydrogen bonds.

The results indicate a strong interaction between CS and AAs in a non-polar environment and a gradual weakening of the interaction in the aqueous phase. These results are significant for modeling the complex penetration process through a cell membrane that is non-polar in nature. The significantly high value of ΔE_{inter} in the gas phase and a very low energy value in the aqueous phase for the complexes indicate its suitability for use in biomedicine.

3.6. The Use of PEC Formed from CS/Collagen To Dye Silk Fabrics with Active and Direct Dyes

We evaluated the influence of the CS/collagen mass ratio of PEC on the colour characteristics of silk fabrics dyed with an active dye in a periodic way in an alkaline medium (Table 4).

Table 4. Influence of the chitosan/collagen mass ratio of polyelectrolyte complexes on the colour characteristics of silk fabric.

No	Chitosan/ collagen mass ratio	Colour indicators							Strength indicators, score	
		K/S	R	L*	A	B	C	h*	To soap	To friction
1	Control (no processing)	0.7	46	81.5	0.3	35.5	35.5	89.6	3/2/2	3/3
2	2:10	1.1	38	78.6	1.7	41.0	41.0	87.6	4/4/4	5/4
3	10:10	1.2	37	78.9	2.2	44.0	44.0	87.1	4/4/4	5/4
4	10:2	1.4	24	72.8	9.2	54.2	55.0	80.4	4/5/5	5/4

The silk fabric dyed with the PEC formed with a CS/collagen mass ratio of 10:2 had the highest colour saturation (C); a pronounced colour tone (h*); the lowest reflectance (R), which indicates an increase in colour intensity; and the lowest brightness values (L*), confirmed by the colour coordinates of the samples.

Colour wheel systems and a colour model are used to systematise the various characteristics of colour and their selection to ensure harmonious colour combinations. Similarly to geographic coordinates, colour values such as L*, a* and b*that is, length, width, and height, respectively – are colour parameters. The L* coordinate characterises the brightness of the colour, the a* coordinate characterises the content of red or green, and the b* coordinate characterises the content of yellow or blue. In this space, colour can also be defined by polar coordinates C* and h*, where C* is colour saturation and h* is colour tone. Based on the results, it follows that the treatment of silk fabric with CS/collagen PEC solutions leads to a change in the colour coordinates – that is, the a* coordinate shifts towards red and the b* coordinate moves from blue to yellow – which contribute to bright and saturated colours.

4. Conclusions

We prepared PEC with several CS/collagen mass ratios. The interaction between CS and collagen occurs through electrostatic interactions and hydrogen bonds of negatively charged functional groups of the macromolecules. When the CS/collagen mass ratio was 10:2, the interaction reached a maximum, which leads to an increase in the particle diameter and diffusion coefficient. We also determined the zeta potential, hydrodynamic dimensions, and the particle diffusion coefficient. We found a relationship between the composition and PEC properties. The results indicate that the colour intensity and saturation of the colour of the dyed natural silk fabric with the active dye was higher in the sample treated with the PEC formed from a CS/collagen mass ratio of 10:2 than in the other samples. We found that when using a CS/collagen mass ratio of 10:2 to dye silk, the colour fastness to soap and friction increased.

5. Acknowledgements

We express our gratitude to I.A. Nabiyeva (Doctor of Technical Sciences, Professor of Tashkent Institute of Textile and Light Industry) for the study of interpolyelectrolyte complexes solutions in the process of dyeing natural silk.

6. References

[1] Krayukhina MA, Samoilova NA, Yamskov IA; (2008) Polyelectrolyte complexes of chitosan: formation, properties and applications. Russ Chem Rev 77, 799. **DOI:**10.1070/rc2008v077n09abeh003750

[2] Kim SE, Cho YW, Kang E J, Kwon IC, Lee EB, Kim JH, Jeong SY; (2001) Three-dimensional porous collagen/chitosan complex sponge for tissue engineering. Fibers Polym 2, 64–70. **DOI:**10.1007/bf02875260

[3] Fernandes LL, Resende CX, Tavares DS, Soares GA, Castro LO, Granjeiro JM; (2011) Cytocompatibility of chitosan and collagen-chitosan scaffolds for tissue engineering. Polímeros 21, 1–6. **DOI:**10.1590/s0104–14282011005000008

[4] Lü X, Zhang H, Huang Y, Zhang Y; (2018) A proteomics study to explore the role of adsorbed serum proteins for PC12 cell adhesion and growth on chitosan and collagen/chitosan surfaces. Regen Biomater 5, 261–273. **DOI:**10.1093/rb/rby017

[5] Quiñones JP, Peniche H, Peniche C; (2018) Chitosan based self-assembled nanoparticles in drug delivery. Polymers 10(3), 235. **DOI:**10.3390/polym10030235

[6] Wu D, Zhu L, Li Y, Zhang X, Xu S, Yang G, Delair T; (2020) Chitosan-based colloidal polyelectrolyte complexes for drug delivery: a review. Carbohydr Polym 238, 116126. **DOI:**10.1016/j.carbpol.2020.116126

[7] Potaś J, Szymańska E, Winnicka K; (2020) Challenges in developing of chitosan-based polyelectrolyte complexes as a platform for mucosal and skin drug delivery. Eur Polym J 140, 110020. **DOI:**10.1016/j.eurpolymj.2020.110020

[8] Li B, Elango J, Wu W; (2020) Recent advancement of molecular structure and biomaterial function of chitosan from marine organisms for pharmaceutical and nutraceutical application. Appl Sci 10(14), 4719. **DOI:**10.3390/app10144719

[9] Do Mai Tran T, Nguyen CT, Quang DoT, Bach GL, Trinh NH, Vu TQ, Thai H; (2020) Preparation and Characterization of Chitosan/Fish Scale Collagen/Lovastatin Nanocomposites. J Polym Environ 28, 2851–2863. **DOI:**10.1007/s10924–020–01819–3

[10] Ahtzaz S, Sher Waris T, Shahzadi L, Anwar Chaudhry A, Ur Rehman I, Yar M; (2019) Boron for tissue regeneration-it's loading into chitosan/collagen hydrogels

and testing on chorioallantoic membrane to study the effect on angiogenesis. Int J Polym Mater Polym Biomat 69(8), 525–534. **DOI:**10.1080/00914037.2019.1581202

[11] Aleem AR, Shahzadi L, Alvi F, Khan AF, Chaudhry AA, ur Rehman I, Yar M; (2017) Thyroxin releasing chitosan/collagen based smart hydrogels to stimulate neovascularization. Mater Des 133, 416–425. **DOI:**10.1016/j.matdes.2017.07.053

[12] Nicolay V, Nina S, Yuliya K, Galina B; (2020) Formation of polyelectrolyte complexes from chitosan and alkaline gelatin, biological resources development and environmental management, KnE Life Sci 5(1), 109–119. **DOI:**10.18502/kls.v5i1.6031

[13] Sun Ch, Yin H, He J, Zou L, Xu Y; (2021) Fabrication and characterization of nanofibrous gelatin/chitosanpoly (ethylene oxide) membranes by electrospinning with acetic acid as solvent. J Polym Res 28, 482. **DOI:**10.1007/s10965–021–02845-y

[14] Jirofti N, Golandi M, Movaffagh J, Ahmadi FS, Kalalinia F; (2021) Improvement of the wound-healing process by curcumin-loaded chitosan/collagen blend electrospun nanofibers: in vitro and in vivo studies. ACS Biomater Sci Eng 7(8), 3886–3897. **DOI:**10.1021/acsbiomaterials.1c00131

[15] Kaur K, Paiva SS, Caffrey D, Cavanagh BL, Murphy CM; (2021) Injectable chitosan/collagen hydrogels nano-engineered with functionalized single wall carbon nanotubes for minimally invasive applications in bone. Mater Sci Eng C 128, 112340. **DOI:**10.1016/j.msec.2021.112340

[16] Valle JAB, Valle R de C S C, Bierhalz A C K, Bezerra FM, Hernandez A L, Lis Arias MJ; (2021) Chitosan microcapsules: methods of the production and use in the textile finishing. J Appl Polym Sci 138(2), 50482. **DOI:**10.1002/app.50482

[17] Rashidova SS, Milusheva RY; (2009) Chitin and chitosan Bombyx mori. Synthesis, properties and application. Publishing House 'FAN', Tashkent.

[18] Temirova, MI, Kodirov, TZ; (2005) Study guide: Technology of leather and fur. Publishing House 'Turon-Iqbol, Tashkent.

[19] Makaseeva ON, Dudinskaya OV, Tkachenko LM; (2003) Proteins. Guidelines for the laboratory workshop on the discipline Biochemistry. MGUP.

[20] Kaldybayeva GY, Nabieva IA, Kaldybayev RT, Nabiev ND, Nurkulov FN, Yeldiyar GK; (2023) Effects of weave structure and water-repellent compositions' formulation on the hydrophobicity property of cotton fabric. Text Res J 0(0), 2023. **DOI**:10.1177/00405175231176496

[21] Shashlov AB, Uarova PM, Churkin AV; (2002) Fundamentals of Lighting Engineering: A Textbook for Universities. MGUP Press, Moscow.

[22] Frisch MJ, Trucks, GW, Schlegel HB, Scuseria GE, Robb MA, Cheeseman JR, Scalmani G, Barone V, Mennucci B, Petersson GA, et al. (2010). Gaussian, Inc., Wallingford CT.

[23] Becke, AD; (1993) Density-functional thermochemistry. III. The role of exact exchange. J Chem Phys 98, 5648–5652. **DOI:**10.1063/1.464913

[24] Galano A, Alvarez-Idaboy JR; (2006) A New approach to counterpoise correction to BSSE. J Comput Chem 27, 1203–1210. **DOI:**10.1002/jcc.20438

[25] Emmanuel M, Pogrebnoi A, Pogrebnaya T; (2015) Theoretical Study of the Interaction between Chitosan Constituents (Glucosamine and Acetylglucosamine Dimers) and Na^+ Ions. Open Access Libr J 2, 1978. **DOI:**10.4236/oalib.1101978

[26] Deka, BC, Bhattacharyya PK; (2015) Understanding chitosan as a gene carrier: A DFT study. Comput Theor Chem 1015, 35–41. **DOI:**10.1016/j.comptc.2014.10.023

[27] Donald JE, Kulp DW, DeGrado WF; (2010) Salt bridges: Geometrically specific, designable interactions. Proteins: Struct Funct Bioinf 79, 898–915. **DOI:**10.1002/prot.22927